

# Understanding uncertainty in temperature effects on vector-borne disease: A Bayesian approach

Leah R. Johnson<sup>\*1,2</sup>, Tal Ben-Horin<sup>3,4</sup>, Kevin D. Lafferty<sup>5,6</sup>, Amy McNally<sup>7</sup>, Erin Mordecai<sup>3,8</sup>,  
Krijn P. Paaijmans<sup>9</sup>, Samraat Pawar<sup>1,10</sup>, Sadie J. Ryan<sup>11,12,13</sup>

1-Ecology and Evolution, University of Chicago; 2-Integrative Biology, University of South Florida;  
3-Ecology, Evolution, and Marine Biology, UC Santa Barbara; 4-Marine and Coastal Sciences, Rutgers University;  
5-Western Ecological Research Center, US Geological Survey; 6-Marine Science Institute, UC Santa Barbara;  
7-Geography Department, UC Santa Barbara; 8-Biology, UNC Chapel Hill;  
9-Barcelona Centre for International Health Research, Universitat de Barcelona;  
10-Department of Life Sciences, Imperial College; 11- Environmental and Forest Biology, SUNY ESF  
12-Center for Global Health and Translational Science, SUNY UMW;  
13 - School of Life Sciences College of Agriculture, Engineering, and Science,  
University of KwaZulu-Natal, Durban, South Africa

**ABSTRACT:** Extrinsic environmental factors influence the distribution and population dynamics  
2 of many organisms, including insects that are of concern for human health and agriculture. This is  
particularly true for vector-borne infectious diseases, like malaria, which is a major source of  
4 morbidity and mortality in humans. Understanding the mechanistic links between environment  
and population processes for these diseases is key to predicting the consequences of climate  
6 change on transmission and for developing effective interventions. An important measure of the  
intensity of disease transmission is the reproductive number  $R_0$ . However, understanding the  
8 mechanisms linking  $R_0$  and temperature, an environmental factor driving disease risk, can be  
challenging because the data available for parameterization are often poor. To address this we  
10 show how a Bayesian approach can help identify critical uncertainties in components of  $R_0$  and  
how this uncertainty is propagated into the estimate of  $R_0$ . Most notably, we find that different  
12 parameters dominate the uncertainty at different temperature regimes: bite rate from 15-25° C;  
fecundity across all temperatures, but especially ~25-32° C; mortality from 20-30° C; parasite  
14 development rate at ~15-16°C and again at ~33-35°C. Focusing empirical studies on these  
parameters and corresponding temperature ranges would be the most efficient way to improve  
16 estimates of  $R_0$ . While we focus on malaria, our methods apply to improving process-based  
models more generally, including epidemiological, physiological niche, and species distribution  
18 models.

**Keywords:** malaria; basic reproductive number; thermal physiology; Bayesian statistics; climate envelope.

# 20 1 Introduction

22 Malaria is a vector-borne disease that is a major source of illness and mortality in humans,  
24 especially in developing countries. Like many vector-borne diseases, the dynamics of malaria are  
26 greatly influenced by extrinsic environmental factors such as temperature and rainfall. As climate  
28 changes over time, the distribution of both epidemic and endemic malaria will likely change as  
well, presenting new challenges for control. A better understanding of how the dynamics of  
malaria depend on environmental factors will be vital for understanding and planning for shifts in  
malaria incidence.

28 Various approaches have been used to try to understand the question of how environmental  
change is likely to impact the prevalence and distribution of malaria [reviewed in Guerra, 2007,  
30 Johnson et al., 2014]. Many of these models can be classified as niche or species distribution  
models, and they seek to link climate factors to observations of the prevalence of vectors,  
32 parasites, or disease occurrence. For mechanistic versions of these models (in contrast to  
geographical correlation models), it is necessary to understand how the vital rates of all players in  
34 disease transmission respond to the environment. Temperature strongly influences vital rates,  
particularly in ectotherms, and its effects can be measured under laboratory conditions. Despite  
36 this basic premise and our reasonable knowledge about thermal physiology, data on responses of  
vital rates to temperature are not widely available. Even for species that have been well studied,  
38 like malarial parasites and their mosquito vectors, the quality and quantity of the data are uneven  
across traits and temperatures. The paucity of data compromises the quality of model predictions,  
40 such as the range of temperatures that are conducive to disease transmission. Moreover, the  
sensitivity of model predictions to errors in empirical estimates is not well known. Here, we  
42 develop methods for estimating sensitivity of model outputs to model inputs, focusing on the  
effect of temperature on malaria transmission.

44 An important and simple measure of transmission, the reproductive number,  $R_0$ , is often used in  
disease studies as it is related to both how quickly a disease can spread in a naïve population and  
46 to the level of prevalence (the proportion of individuals that have been infected) for endemic

diseases [Keeling and Rohani, 2008]. Recently, approaches have been developed to model how  
48  $R_0$  depends on temperature by incorporating thermal responses of traits underlying  $R_0$ , such as  
mosquito and parasite development rates [Mordecai et al., 2013, Molnár et al., 2013]. For malaria,  
50 the method involves the use of laboratory data collected on the temperature dependence of all  
components of  $R_0$  that depend upon parasite or vector physiology — temperature response curves  
52 fitted to each component are incorporated into the  $R_0$  equation to find the overall thermal  
dependence of transmission. Including these physiologically based thermal responses produces  
54 predictions of transmission that are more inline with observed incidence patterns than previous  
models that do not incorporate these detailed physiological responses, even without accounting  
56 for rainfall [Mordecai et al., 2013]. Although many other factors, such as key control measures,  
may better predict malaria morbidity and mortality, this kind of relatively simple modeling is a  
58 promising first step in prioritizing global health policy to respond to broad changes in the spread  
and intensification of infectious diseases [Altizer et al., 2013].

60 Empirical research on the factors or components that determine  $R_0$  is costly. Thus, it is important  
to direct future research towards aspects that will result in the greatest reduction in uncertainty in  
62  $R_0$  overall, and thus improve our predictions of changes in future transmission the most.

Currently, the laboratory data necessary to understand the temperature dependence of the  
64 components that determine the response of  $R_0$  to temperature are often limited. Available data  
leave substantial uncertainty about the relationship between each component of  $R_0$  and  
66 temperature, especially at the temperatures that are marginal for transmission. Thus, we anticipate  
considerable uncertainty in how  $R_0$  varies with temperature. By better understanding all of the  
68 sources of uncertainty we can prioritize laboratory studies more efficiently and design effective  
intervention strategies [Elder et al., 2006, Merl et al., 2009]. Mordecai et al. [2013] addressed  
70 this issue to some degree by performing a sensitivity analysis by perturbing the  $R_0$  components  
with respect to temperature. However, this kind of simple, single-parameter local sensitivity  
72 analysis does not allow a full understanding of either the uncertainty in components or in  $R_0$   
overall. Further, additional data on components of  $R_0$  for closely related species or less

74 well-controlled experiments are often available. These additional data, even if not ideal for fitting  
the final models directly, can be informative.

76 Here we use a Bayesian approach [Clark, 2007] to understand the full range of uncertainty in the  
thermal response of malarial  $R_0$ . The focus of a Bayesian analysis is the posterior distribution:  
78 i.e., the probability that the parameters have some value given the data. This is obtained by  
combining a likelihood (the probability of observing the data given parameters with particular  
80 values) and a prior distribution (the assumed probability that the parameters have some values  
independent of the observed data) using Bayes rule. A full discussion of the Bayesian approach  
82 can be found elsewhere [e.g. Clark, 2007]. A Bayesian approach allows us to incorporate prior  
knowledge about the various components of  $R_0$ , for instance, by using data from related species  
84 in the inference procedure. This is especially useful in applications that rely heavily on sparse  
data, such as the one explored here.

86 We are interested in two primary aspects of the relationship between transmission and  
temperature: (1) which temperatures prevent transmission? and (2) which temperatures promote  
88 transmission? Earlier work on temperature and disease transmission in general, and for malaria in  
particular, has produced mixed results, in part because the impact of temperature on preventing  
90 transmission (as opposed to promoting it) is often ignored [Rohr et al., 2011, Hay et al., 2002,  
Siraj et al., 2014, Gething et al., 2010]. We use a Bayesian approach to explore the uncertainty  
92 and sensitivity of these two transmission outcomes – prevention and promotion – to mosquito and  
parasite traits.

94 We begin by introducing the  $R_0$  model and its components, the potential thermal responses for all  
its components, and the available data on these thermal responses. We then introduce the data  
96 model, initial “uninformative” priors, and our overall methodology. We then step through a series  
of uncertainty and sensitivity analyses, together with the results for each analysis. This is  
98 followed by a discussion of how the approach taken compares to more classical analyses, and the  
implications of the results.

## 2 Data, Models, and Methods

The standard model of malaria transmission by a vector is the Ross-McDonald model [Macdonald, 1952], from which the reproductive number  $R_0$  is derived.  $R_0$  determines the dynamical threshold for disease transmission, and is defined as the average number of secondary infections caused by a single infected individual in an entirely susceptible population. It specifies the relationships of parameters in the model that are required for an infection to spread within a population ( $R_0 > 1$ ) as opposed to dying out ( $R_0 < 1$ ). The most widely used formulation for malarial  $R_0$  [Dietz, 1993] is

$$R_0 = \sqrt{\frac{M a^2 bc \exp(-\mu/PDR)}{Nr \mu}}, \quad (1)$$

where  $M$  is the density of mosquitoes,  $a$  is the bite rate,  $bc$  is vector competence,  $\mu$  is the mortality rate of adult mosquitoes,  $PDR$  is the parasite development rate ( $1/EIP$ , the extrinsic incubation period of the parasite),  $N$  is the human density, and  $r$  is the human recovery rate. Most of these model components are directly measurable or are closely related to quantities or traits that can be observed [Mordecai et al., 2013]. Following Mordecai et al. [2013], we assume that the expected mosquito density is given by:

$$M = \frac{EFD p_{EA} MDR}{\mu^2}, \quad (2)$$

where  $EFD$  is number of eggs produced per female per day,  $p_{EA}$  is the probability that an egg will hatch and the larvae will survive to the adult stage, and  $MDR$  is the mosquito development rate. The parameters that jointly define  $R_0$  and  $M$  are summarized in Table 1, and throughout this paper we refer to these as “components of  $R_0$ ”.

Virtually all physiological traits in ectotherms exhibit unimodal temperature responses, i.e., they have an optimal temperature at which the trait is maximized, and declines on either side [e.g.,

Amarasekare and Savage, 2012, Dell et al., 2011, Angilletta, 2009]. However, the exact functional

form of the unimodal response is still under debate, especially because it is known to vary with  
122 the type of trait [Dell et al., 2011, Mordecai et al., 2013]. Therefore, as in Mordecai et al. [2013],  
we determined the appropriate thermal-response model for each component trait by fitting  
124 candidate functional forms: quadratic for symmetric responses and Briere for asymmetric (see  
Section 2.2.1 and Figure 1). These were chosen as they are among the simplest functional forms  
126 that exhibit the desired unimodal behavior.

All analyses were conducted in R [R Development Core Team, 2008] with Markov chain Monte  
128 Carlo (MCMC) implemented in `rjags/JAGS` (Just Another Gibbs Sampler, [Plummer, 2003,  
2013]). Computer code for all analyses are included in the Supplementary Files.

## 130 **2.1 Data**

We use two sets of data in our analysis — the “main” dataset contains the focal data for the  
132 thermal responses for the components that make up  $R_0$  (Table 1), and a “prior” dataset used to  
elicit priors for our Bayesian analysis (both sets included in the Supp. Files; for sources see  
134 Supp. App. A, Table 1). Ideally, our main data set would exclusively comprise laboratory data on  
*Plasmodium falciparum*, the causative agent of the majority of tropical malaria, and its primary  
136 vector *Anopheles gambiae*, held at constant temperature for all components. These data were  
available for only three traits: mosquito development rate (MDR), egg to adult survival ( $p_{EA}$ ), and  
138 adult mosquito mortality rate ( $\mu$ ). For other traits ideal data are unavailable [Mordecai et al.,  
2013], and instead we used data from related species collected under appropriate laboratory  
140 conditions. More specifically, we prioritized data collected in the laboratory at constant  
temperatures. For mosquito and parasite traits, we prioritized based on the relative to efficacy of  
142 transmission and severity of disease in humans. Thus, for mosquito traits, we prioritized data for  
*An. gambiae*, followed by other anophelene species, and finally for *Aedes* species. For parasite  
144 traits, *P. falciparum* was prioritized, followed by *P. vivax*. When possible, only a single mosquito  
or parasite species was used for an individual trait in the main data. For our prior data set, our  
146 conditions for inclusion were more flexible. Although data on related species held in the lab at

constant temperature were preferred, we also allowed more distantly related species, or less  
148 controlled (variable temperature) experiments. These data are distinct from the main data set and  
were used, along with expert opinion, to elicit informative priors for the parameters of the  
150 unimodal temperature responses for each  $R_0$  component.

## 2.2 Approach, Likelihoods, and Priors

152 We fitted the thermal response of each component of  $R_0$  (Table 1) to independent data using a  
Bayesian approach to obtain the posterior distribution for the parameters that describe each  
154 response (and thus the posterior distribution of the response itself), as well as for  $R_0$  overall.  
Inference in the Bayesian framework proceeds in three steps. First, a likelihood is defined for  
156 each type of data. Second, appropriate prior distributions are determined. Third, samples from the  
posterior distribution of the parameters, given the data, are obtained via Markov-chain Monte  
158 Carlo (MCMC). We used this procedure first for the prior data and for the main data, assuming  
uninformative priors in both cases (Section 2.2.2 and Supp. App. A Section 2). Next, the posterior  
160 distributions obtained from analyzing the prior data were used to build informative priors and the  
inference procedure was repeated for the main data using these informative priors. We then  
162 compared the resulting posterior distributions obtained using the uninformative and informative  
priors. Further, we calculated  $R_0$  with both sets of results, and compared these. This gave an  
164 indication of the sensitivity of the individual components and of  $R_0$  to the choice of prior. We  
followed this with further sensitivity and uncertainty analyses (Section 3).

### 2.2.1 Likelihoods

We assumed functional forms for each component based on our previous work [Mordecai et al.,  
168 2013] and on the types of functional forms (unimodal and frequently asymmetric) that are typical  
for similar traits in other arthropod species [Dell et al., 2011]. More specifically, we used either a  
170 quadratic (symmetric) or Briere (asymmetric) function, depending on the component. At any  
given temperature, the mean response should be determined by this functional form. Further, all  
172 model components are, by definition, greater than or equal to 0. Thus, we chose to use a truncated

normal distribution, with mean parameter (usually denoted by  $\mu$ ) given by the appropriate  
174 functional form (i.e., Briere or quadratic), as the likelihood for the data for most of the  
components of  $R_0$ . For all of the components we examined, the lower truncation limit was at zero.  
176 Most components can take any value greater or equal to zero. Thus, for most of our data  
 $Y_i | 0 < Y_i < b \stackrel{iid}{\sim} N(\mu = f(T_i), \sigma^2)$ , where  $b$  is the upper truncation limit (either 0 or  $\infty$ ),  $f(T_i)$  is  
178 the Briere or quadratic temperature response, and *iid* indicates that the data are independently and  
identically distributed. However, two components, the vector competence (*bc*) and the egg to adult  
180 survival ( $p_{EA}$ ), are probabilities and are thus constrained to be between zero and one. For these  
components, we would ideally have the actual numbers of successes and total numbers of  
182 observations so that the more appropriate binomial model could be used. These data were indeed  
available for vector competence, and so were modeled with a binomial likelihood, i.e.  
184  $Y_i \stackrel{iid}{\sim} \text{Bin}(n, p = f(T_i))$ , where  $n$  is the number of total observations, of which  $Y$  were successes,  
and the probability,  $p$  of a success at a particular temperature,  $f(T_i)$ , is either Briere or quadratic.  
186 For egg to adult survival the raw data were not available so we used a normal distribution  
truncated at zero and one to model the proportion of eggs that successfully mature to the adult  
188 stage. This choice keeps calculations simple, allows straightforward implementation of  
biologically based priors, and has shape properties that are more appropriate for these data than  
190 alternatives such as a beta distribution.

### 2.2.2 Priors

192 We began by defining a set of default priors for all parameters that are chosen to be relatively  
“uninformative”. That is, these priors were designed to constrain parameter values to be  
194 biologically reasonable, but to otherwise provide wide, reasonably even support across potential  
parameter values. In particular, for our default priors, we assumed that the maximum temperature  
196 at which a unimodal, hump-shaped component goes to zero is 45°C, and the minimum  
temperature should be 0°C, as these temperatures are generally lethal to mosquitoes. This upper  
198 limit is slightly higher than some observed upper lethal limits, which are closer to 40°C [Bayoh,  
2001, Bayoh and Lindsay, 2003, Lardeux et al., 2008]. We chose the higher, conservative, limit to



200 allow a broader range of temperatures for which the data could inform the posterior distributions.  
Each of the concave-down (or hump-shaped) curves have a parameter that describes the  
202 temperatures at which trait goes to zero, notated as  $T_0$  and  $T_m$  for the lower and upper limits,  
respectively. Since we required  $T_0 < T_m$  we specified non-overlapping priors for these  
204 parameters. For the concave-up quadratic we chose priors that limited the quadratic curves to  
those that are concave up and in the appropriate quadrant. We set the priors on other parameters  
206 (including the precision parameter,  $\tau = 1/\sigma$ , in the normal distribution) to be diffuse, i.e., to have  
wide support. Details can be found in Supp. App. A, Sections 2 and 3. In all cases we examined  
208 the sensitivity of the posterior distributions to the priors.

### 3 Uncertainty and Sensitivity Analyses and Results

210 Our uncertainty and sensitivity analyses consisted of multiple parts. First, we addressed sources  
of uncertainty in our analysis, to understand the expected response of  $R_0$  and its components to  
212 temperature, and the range of responses that are supported by data. This is similar to global  
sensitivity analysis for the components and  $R_0$ . Our measure of uncertainty for each analysis is  
214 the 95% highest probability density (HPD) interval which gives the range of a parameter or  
response corresponding to a central area containing 95% of the probability. Second, we compared  
216 how the uncertainty in  $R_0$  overall depends on the uncertainty in its components, using a variant of  
local sensitivity analysis, and comparing the results to those obtained for the global-style analysis.  
218 Third, we addressed how sensitive  $R_0$  is to temperature and to its components, as well as the  
uncertainty in these relationships. Here, sensitivity is the amount by which  $R_0$  changes when  
220 temperature changes, and is given by the derivative of  $R_0$  with respect to  $T$ . As with  $R_0$  itself, the  
uncertainty in this sensitivity is expressed in terms of the 95% HPD intervals. How the Bayesian  
222 and classical approaches to these analyses compare is addressed further in the discussion.

### 3.1 Uncertainty in the components of $R_0$

224 **How uncertain are the responses of the mosquito and parasite traits to temperature, and**  
225 **how does this depend on the prior information included in the analysis?**

226 To answer this question we made three sets of comparisons. First, we qualitatively examined the  
227 impact of adjusting the default priors for each parameter on the inference for individual  
228 components (with both the main and prior data). Second, we compared the posterior distributions  
229 for individual components of the main data set obtained with default and informative priors. In  
230 this case, the informative priors are generated from the posterior distributions obtained from  
231 fitting the prior data to elicit informative priors. Third, we examined the impact of using an  
232 alternative functional response for the vector competence term, for which there is both relatively  
233 little data and little *a priori* support for a particular functional form.

234 The impact of including the informative priors varied between components, in some cases  
235 decreasing uncertainty (smaller HPD intervals around the mean –  $bc$ ,  $p_{EA}$ ,  $EFD$ ,  $PDR$ ),  
236 sometimes increasing uncertainty (larger HPD intervals around the mean –  $a$ ,  $MDR$ ), or having  
237 little impact on the posterior (no change in HPD intervals –  $\mu$ ) (Supp. App. B, Section 1). Across  
238 components, modifying priors on the lower and upper temperature limits of the responses ( $T_0$  and  
239  $T_m$ , respectively) had the greatest impact on the posterior distributions of the temperature  
240 responses overall. The upper limit of 45°C on  $T_m$  for the default and some of the informative  
241 priors was important for components for which no high temperature data were available, such as  
242 the bite rate,  $a$ . Full results for each component, including inferences with both types of priors,  
243 and a comparison of the marginal posterior distributions of parameters with their priors, are  
244 included in Supp. App. B.

245 In Figure 1 we show the posterior mean and 95% HPD interval around this mean (summarizing  
246 the extent of our uncertainty around this response) for all the components when informative priors  
247 were used. Some interesting patterns emerged when we compared across components. First, for  
248 all components modeled with a Briere function (top row of Figure 1), the low temperature limit  
(the temperature below which the trait is zero) was less certain than the upper temperature limit

250 (although this difference was small for PDR). This was partly due to the nature of the functional  
form – i.e., it goes to zero more quickly at high temperatures than it does at low temperatures.  
252 However, it also reflected that there were often fewer data available across lower temperatures  
than high temperatures in the main and prior data together. This pattern of uncertainty at the  
254 limits was not found for the concave down quadratic responses (middle row, Figure 1). Instead, in  
some cases, the upper limit was less certain than the lower. This indicates that the temperature  
256 resolution for experiments needed to pin down the responses may depend on the type of response  
(asymmetric vs. symmetric) that a trait exhibits.  
258 For most of the components explored, either the data gave a strong indication of whether a  
symmetric or asymmetric response was appropriate [Mordecai et al., 2013], or there were  
260 biophysical reasons why we expected a response to be asymmetric or symmetric *a priori*  
[Angilletta, 2009, Dell et al., 2011]. However, vector competence (a compound trait) was  
262 ambiguous. Thus, we fit both a quadratic and Briere function for this component. Both fit quite  
well, and thus the impact of fits using both functional forms on the uncertainty in  $R_0$  was  
264 addressed in the subsequent analysis.

### 3.2 Overall uncertainty in $R_0$

266 **How uncertain is the response of the basic reproductive rate,  $R_0$ , to temperature (due to  
uncertainty in all components), and how does this depend on the prior information included  
268 in the analysis?**

To answer this question we made three comparisons. First, we compared the posterior  
270 distributions of  $R_0$  under default and informative priors for the components, looking at the overall  
uncertainty (95% HPD interval) of the full response curve when all components were allowed to  
272 vary according to their posterior distributions. Second, we examined the HPD intervals of three  
important summaries of  $R_0$ : minimum (low temperature transmission limit), maximum (high  
274 temperature transmission limit), and peak (temperature at maximal transmission)  $R_0$ . Third, we  
examined the impact of the two functional responses for the vector competence term on the

276 posterior distribution of  $R_0$ . This analysis shows the overall uncertainty around (1) which  
temperatures prevent transmission (low and high temperature transmission limits) and (2) which  
278 temperatures promote transmission (peak temperature).

In Figure 2 (top) we show the posterior mean of the temperature dependence of  $R_0$  and 95% HPD  
280 intervals of the temperature response of  $R_0$  when both informative and uninformative priors are  
used. All curves are scaled to the maximum value of the mean  $R_0(T)$  curve. These are generated  
282 using posterior samples from all components, and so indicate the overall uncertainty in the  
response curve due to uncertainty in all components, simultaneously. Notice that the mean  $R_0$   
284 curves obtained using default and informative priors are very similar. Further, the upper 95%  
HPD intervals were nearly identical. However, the lower HPD intervals of  $R_0$ , especially at higher  
286 temperatures, differ considerably as the additional prior information allowed us to pin down the  
high temperature transmission limit more precisely. This can be seen more clearly by looking at  
288 the posterior distributions of the upper and lower temperature limits of  $R_0$  and the distribution of  
the temperature at peak  $R_0$  (Figure 2, bottom). With the default priors, almost the full range of  
290 possibilities for the lower (from 0 to 24 °C) and upper (from 25 to 45 °C) limits were equally  
represented. Adding in prior information indicates support for a slightly lower temperature limit  
292 to malaria transmission while the upper limit is at a slightly higher temperature than was predicted  
with default priors. In other words, the climate envelope where transmission may be possible is  
294 slightly larger than would be inferred without prior data. Further, our estimates of the  
temperatures that can exclude malaria, particularly at the upper end, are more precise. However,  
296 the prediction of the temperature of peak transmission, which corresponds to temperatures at  
which malaria is expected to be most severe and difficult to control, was robust.

298 As mentioned in the previous section, the most appropriate functional response to describe the  
temperature dependence of vector competence ( $bc$ , a compound trait) was ambiguous. Since both  
300 functional forms fit the available data well, we examined how using each impacted the posterior  
inferences for  $R_0$ . To do this, we calculated  $R_0$  using first the posterior samples for the Briere  
302 response for  $bc$  and then the quadratic. All other components of  $R_0$  were allowed to take all

possible values of their posterior distributions. Thus our comparison shows how the uncertainty in  
304 the functional form for  $bc$  impacts the overall uncertainty in  $R_0$  given the full uncertainty in the  
other parameters. The choice of the functional form for  $bc$  had little impact on the the posterior  
306 distribution of  $R_0(T)$  except at the high temperature limit (Supp. App. B). As with other  
components examined, the vector competence fit with a Briere function exhibited reduced  
308 uncertainty in the upper limit compared to the quadratic fit, and as a result decreased the  
uncertainty in  $R_0$  at this limit. Since there is no *a priori* reason to prefer one or the other of these,  
310 in all further analyses we assumed the quadratic fit, as this resulted in the most uncertainty in  $R_0$   
at the upper limit, and was thus a more conservative choice.

### 312 **3.3 Uncertainty in $R_0$ and its sensitivity to temperature, by component**

**Which mosquito and parasite traits drive the uncertainty in  $R_0$ , across temperatures?** To  
314 answer this question, we used a variation of a traditional sensitivity analysis. We set all but a focal  
component to its posterior mean. Then the posterior samples of the focal component were used to  
316 calculate the width of the 95% HPD at each temperature due to only the variation in this single  
component. We then normalized this to the width of the 95% HPD for the full posterior of  $R_0$   
318 (i.e., when all components were allowed to vary) to approximate the proportion of the uncertainty  
each component contributed to the full uncertainty in  $R_0$ .

320 In Figure 3 (a) we show the amount of uncertainty in  $R_0$  due to a single component, compared to  
the uncertainty overall. The adult mosquito mortality rate  $\mu$ , dominated at intermediate  
322 temperatures, i.e., the region in which temperature promotes transmission, because  $R_0 \propto 1/\mu^3$   
(by definition from Equations (1) and (2)), and at intermediate temperatures the rate of adult  
324 mosquito mortality is low. More surprising was the relatively narrow range of temperatures where  
it dominated:  $\mu$  dominated in the middle third of the transmission range, and is primarily  
326 determined the height and location of peak  $R_0$ . This explains why the informative priors had so  
little impact on the upper HPD interval for  $R_0$  (Figure 2) – the posterior of  $\mu$  was not impacted by  
328 additional prior information and this component determined the height of the curve. By contrast,

the uncertainty on the lower and upper limits for transmission was driven by bite rate and  
330 fecundity, respectively. In particular, uncertainty in the bite rate ( $a$ ) drove uncertainty in the lower  
temperature boundary, while the fecundity ( $EFD$ ), was most important at the upper temperature  
332 limit. These two components were also the most important sources of uncertainty, after  $\mu$ , at  
intermediate temperatures. Other components, such as vector competence ( $bc$ ), contributed very  
334 little to the overall uncertainty, despite the fact that the data on these components were sparse.  
This was primarily because parameters like this are probabilities, bounded between zero and one,  
336 and only impact  $R_0$  proportionally. Other parameters have the potential to vary over orders of  
magnitude, and thus swamp the impact of these parameters over most of the range of  $R_0$ . Only  
338 when the magnitude of the other parameters are small, such as the temperature extremes, can  
these contribute significantly to the overall uncertainty.

340 **Which mosquito and parasite traits determine the sensitivity of  $R_0$  to temperature and the  
uncertainty in the sensitivity, across temperatures?** Next we examined how sensitive  $R_0$  is to  
342 changes in temperature, that is, how various components contribute to the *change* in  $R_0$  with  
temperature, as measured by the derivative of  $R_0$  with respect to temperature. We especially  
344 focused on the uncertainty of the sensitivity, measured by the HPD interval around the mean  
sensitivity, and which components drive the uncertainty. We focus on these as they indicate the  
346 data that can best help improve our understanding of what determines the shape of  $R_0$  across  
temperatures. We started with a standard sensitivity analysis, calculating the derivative of  $R_0$  with  
348 respect to temperature overall and for each component separately,  $\left(\frac{dR_0}{dT}\right)_\theta$  (see Supp. App. A  
Section 5 for equations). As with the previous analysis, we then set all components, save a focal  
350 component to its mean, and used the posterior samples from that focal component to obtain the  
marginal posterior distribution for the sensitivity. We repeated this for all components, then  
352 examined the median sensitivity and the width of the 95% HPD intervals for the component-wise  
sensitivity,  $\left(\frac{dR_0}{dT}\right)_\theta$ , relative to the overall sensitivity,  $\frac{dR_0}{dT}$  (calculated using the posterior samples  
354 from all the components at once) to see which components were driving the sensitivity of  $R_0$  to  
temperature and the uncertainty in the sensitivity.

356 In Figure 3 (b) we show the uncertainty in the sensitivity of  $R_0$  to temperature by each component  
scaled by the overall uncertainty in the sensitivity of  $R_0$  to temperature. For instance, the median  
358 sensitivities, by component, indicate that at low temperatures  $R_0$  was very sensitive to the bite rate  
and at high temperatures (even the very highest) the mortality rate drove the response of  $R_0$  to  
360 temperature (Supp. App. C). However, at very high and very low temperatures, other components  
besides bite rate and mortality began to be important as well, and these other components were  
362 less certain. Thus, at the temperature extremes determining where transmission is not possible,  
the *uncertainty* in how sensitive  $R_0$  is to temperature was driven by other components, such as  
364 fecundity (EFD) and the parasite development rate (PDR).

## 4 Discussion

366 Using a Bayesian approach, we identified component traits that were the main sources of  
uncertainty in  $R_0$ , and in how sensitive  $R_0$  is to temperature. Overall, uncertainty about the  
368 temperature limits on transmission was greater than the uncertainty in the optimal temperature for  
transmission. We found that much of the uncertainty in  $R_0$  was due to adult mosquito mortality,  $\mu$ ,  
370 as one would expect given  $R_0$ 's nonlinear dependence on mortality. This contribution was focused  
in the region of temperatures that promote transmission, where  $\mu$  and its uncertainty were small.  
372 Other components determined the uncertainty near the temperature limits of  $R_0$  in terms of the  
relative width of the HPD intervals. In particular, near the low temperature limit, the uncertainty  
374 in  $R_0$  was largely due to uncertainty in the bite rate,  $a$ , whereas near the high temperature limit the  
uncertainty was primarily due to uncertainty in fecundity (EFD). Fecundity also contributed a  
376 relatively large amount of uncertainty across temperatures. The uncertainty in the high  
temperature limit itself was determined primarily by the parasite development rate (PDR).

378 The most important empirical data needed to improve model certainty depends on the goals. To  
resolve the uncertainty in the temperature optimum, empirical studies should focus on measuring  
380 adult mosquito mortality rate from 20-30° C, as well as bite rate and fecundity. By contrast,  
resolving uncertainty surrounding the lower and upper temperature limits on transmission

382 requires measuring 1) bite rate from 15-25° C; 2) fecundity across temperatures, but especially  
~25-32° C; and 3) PDR at ~15-16° C and 33-35° C. This last is especially interesting, because  
384 PDR is not driving the overall uncertainty at any temperature. Instead, our uncertainty in how  
*sensitive*  $R_0$  is to temperature depends on PDR at both temperature extremes. More specifically,  
386 our uncertainty in the temperature at which  $R_0$  changes from zero is driven by PDR,. This also  
suggests that PDR component could be determining the temperature limits for malaria  
388 transmission, and the ability of the parasite to evolve at the edges of its thermal limits could  
determine where malaria could occur. Resolving the temperature limits is particularly important  
390 given that warming is expected to expand transmission into currently or recently unsuitable  
highland areas [Siraj et al., 2014], and may force currently warm, suitable lowland areas above the  
392 upper transmission limit. Differences in the presumed thermal limits that inhibit transmission can  
impact predictions of when and where transmission is likely to occur both now and in the future.  
394 [Ryan et al., Submitted]. A better understanding of the uncertainty in the temperatures that inhibit  
transmission should help inform policy priorities as climate changes.

396 Further, our results provide guidance as to which components may not be as high priority for  
further work. For instance, our analysis indicates which components are contributing relatively  
398 little to the uncertainty in  $R_0$ , such as vector competence (*bc*). Although these components are  
necessary for transmission (incompetent vectors cannot transmit disease, for example),  
400 investment in reducing uncertainty in these components will have a comparatively small impact  
on our overall understanding of  $R_0$ . Thus, these components could be given a lower priority for  
402 further empirical effort, especially if these components are difficult or expensive to measure.

Our method is unusual in that it combines concepts and approaches from traditional global and  
404 local sensitivity analyses with a Bayesian method of inference. Bayesian analyses often focus on  
the inference and uncertainty aspects, and, for simpler models, model and variable selection. If  
406 sensitivity is addressed, it is typically the sensitivity of the posterior to the prior specification.  
Conversely, most sensitivity analyses would typically be conducted using parameter values  
408 selected at random or evenly over some “reasonable range” of parameters for a system instead of



performing parameter inference as part of the procedure. This traditional approach would be most  
410 similar to performing our analysis using samples from informative priors. The choice to take the  
extra step and fit data before doing the uncertainty and sensitivity analyses depends on whether or  
412 not appropriate, high quality data are available for the analysis. If this is not the case, then  
incorporating additional data could lead to bias in results. However, even moderately good data,  
414 such as we have in our example, allowed us to narrow down the regions of parameter space that  
are reasonable for our system by allowing the data to inform us of how the parameters that  
416 describe our thermal response curves are correlated for each component of  $R_0$ , which is not easy  
to obtain *a priori*.

418 On the other hand, in this example, we have been forced to use data from alternative species, even  
for the focal data. For instance, we used fecundity data for *Aedes albopictus* for the focal data,  
420 even though we expect these are likely to be different from any *Anopheles* species. We also used  
*P. vivax* data for vector competence. Thus, we may have underestimated the overall uncertainty in  
422  $R_0$  and the uncertainty due to these components. It is unclear how to explicitly incorporate this  
into the current (or any other) framework to quantify the impact of using these data. However, the  
424 types of sensitivity analyses we conducted take into account the structure of the model, and give  
information about how much each component could potentially contribute to the overall  
426 uncertainty. We can, therefore, use these analyses to complement our intuition about how to focus  
research efforts. Thus, although fecundity for Anophelene species and vector competence for  
428 *P. falciparum* could be useful (since we had to use alternative species for these analyses), when  
combined with the rest of the analyses, we would prioritize fecundity as uncertainty in that  
430 component has a bigger impact on overall uncertainty. Further, we might expect that some  
components that contribute to  $R_0$  have biological reasons to be more uncertain, for instance  
432 because there is more individual variability in some traits or local adaptation [Sternberg and  
Thomas, 2014]. With appropriate data we could explicitly include individual (or population) level  
434 variation as part of the analysis, or combine data across different populations while allowing  
differences in thermal response curves within the framework.

436 Although we applied our methods to a particular formulation of  $R_0$  for malaria, the approach is  
appropriate for mechanistic models of other systems, including other vector-borne disease and  
438 species distribution models. To best understand the full uncertainty for a particular disease or  
species distribution, consideration of multiple mechanistic models and environmental drivers  
440 would allow researchers to further understand model uncertainty, and the robustness of  
predictions to other formulations. For instance, alternative dynamical models could change the  
442 estimate of the peak and range of species distributions as the functional relationship between  
various traits or vital rates and population performance could be substantially different. This is an  
444 issue that is largely ignored in the literature addressing disease incidence, species distributions,  
and climate envelopes. This source of model uncertainty needs to be addressed to fully quantify  
446 uncertainty in the response of populations to climate change. We suspect that for many species  
and diseases, including malaria, the uncertainty inherent in the individual components would  
448 often swamp model uncertainty in big picture quantities like  $R_0$ . This is especially true when data  
from a focal species are not available at all, as discussed above, and further emphasises the  
450 importance of high quality data for parameterising these kinds of models. However, alternative  
formulations incorporate each component in different ways, so the conclusions about which  
452 components drive uncertainty are likely to be less robust. Consideration of multiple models can  
indicate what data acquisition should be prioritized, for instance if it is important across a variety  
454 of model formulations, and further, which new data would allow better discrimination between  
competing models. The Bayesian approach allows direct comparison of models and their  
456 uncertainty. Thus it has the potential to be a useful tool for identifying concrete recommendations  
for future research to improve predictions of how factors such as climate change could impact the  
458 distribution of malaria and other vector-borne diseases.

**Acknowledgements:** This work was conducted as part of the Malaria and Climate Change  
460 Working Group supported by the Luce Environmental Science to Solutions Fellowship and the  
National Center for Ecological Analysis and Synthesis, a Center funded by NSF (EF-0553768),  
462 the University of California, Santa Barbara and the State of California. EAM was funded by an

NSF Doctoral Dissertation Improvement Grant (DEB-1210378), and an NSF Postdoctoral

464 Research Fellowship (DEB-1202892). Any use of trade, product or firm names in this publication  
is for descriptive purposes only and does not imply endorsement by the US government.

## 466 **References**

S. Altizer, R. S. Ostfeld, P. T. Johnson, S. Kutz, and C. D. Harvell. Climate change and infectious  
468 diseases: From evidence to a predictive framework. *Science*, 341(6145):514–519, 2013.

P. Amarasekare and V. Savage. A framework for elucidating the temperature dependence of  
470 fitness. *The American Naturalist*, 179(2):178–191, Feb. 2012.

M. J. Angilletta. *Thermal adaptation: a theoretical and empirical synthesis*. Oxford University  
472 Press, 2009.

M. Bayoh and S. Lindsay. Effect of temperature on the development of the aquatic stages of  
474 *Anopheles gambiae* sensu stricto (diptera: Culicidae). *Bulletin of entomological research*, 93  
(5):375–382, 2003.

476 M. N. Bayoh. *Studies on the development and survival of Anopheles gambiae sensu stricto at  
various temperatures and relative humidities*. PhD thesis, Durham University, 2001.

478 J. S. Clark. *Models for Ecological Data*. Princeton University Press, Princeton, NJ, 2007.

A. I. Dell, S. Pawar, and V. M. Savage. Systematic variation in the temperature dependence of  
480 physiological and ecological traits. *Proceedings of the National Academy of Sciences*, 108(26):  
10591–10596, June 2011.

482 K. Dietz. The estimation of the basic reproduction number for infectious diseases. *Statistical  
Methods in Medical Research*, 2(1):23–41, Mar. 1993.

484 B. D. Elderd, V. M. Dukic, and G. Dwyer. Uncertainty in predictions of disease spread and public  
health responses to bioterrorism and emerging diseases. *Proceedings of the National Academy*

486 *of Sciences*, 103(42):15693–15697, 2006. doi: 10.1073/pnas.0600816103. URL  
http://www.pnas.org/content/103/42/15693.abstract.

488 P. W. Gething, D. L. Smith, A. P. Patil, A. J. Tatem, R. W. Snow, and S. I. Hay. Climate change  
and the global malaria recession. *Nature*, 465(7296):342–345, May 2010.

490 C. A. Guerra. *Mapping the contemporary global distribution limits of malaria using empirical  
data and expert opinion*. PhD thesis, University of Oxford, Sept. 2007.

492 S. I. Hay, J. Cox, D. J. Rogers, S. E. Randolph, D. I. Stern, G. D. Shanks, M. F. Myers, and R. W.  
Snow. Climate change and the resurgence of malaria in the east african highlands. *Nature*, 415  
494 (6874):905–909, 2002.

L. R. Johnson, K. D. Lafferty, A. McNally, E. A. Mordecai, K. P. Paaijmans, S. Pawar, and S. J.  
496 Ryan. Mapping the distribution of malaria: current approaches and future directions. In  
D. Chen, B. Moulin, and J. Wu, editors, *Analyzing and Modeling Spatial and Temporal  
498 Dynamics of Infectious Diseases*. John Wiley & Sons, 2014.

M. J. Keeling and P. Rohani. *Modeling infectious diseases in humans and animals*. Princeton  
500 University Press, Princeton, 2008.

F. Lardeux, R. Tejerina, V. Quispe, and T. Chavez. A physiological time analysis of the duration  
502 of the gonotrophic cycle of *Anopheles pseudopunctipennis* and its implications for malaria  
transmission in Bolivia. *Malaria journal*, 7(1):141, 2008.

504 G. Macdonald. The analysis of equilibrium in malaria. *Tropical diseases bulletin*, 49(9):813,  
1952.

506 D. Merl, L. R. Johnson, R. B. Gramacy, and M. Mangel. A statistical framework for the adaptive  
management of epidemiological interventions. *PLoS ONE*, 4(6):e5807, 06 2009. doi:  
508 10.1371/journal.pone.0005807. URL  
http://dx.doi.org/10.1371%2Fjournal.pone.0005807.

510 P. K. Molnár, S. J. Kutz, B. M. Hoar, and A. P. Dobson. Metabolic approaches to understanding  
climate change impacts on seasonal host-macroparasite dynamics. *Ecology Letters*, 16(1):921,  
512 2013.

E. A. Mordecai, K. P. Paaijmans, L. R. Johnson, C. Balzer, T. Ben-Horin, E. de Moor,  
514 A. McNally, S. Pawar, S. J. Ryan, T. C. Smith, and K. D. Lafferty. Optimal temperature for  
malaria transmission is dramatically lower than previously predicted. *Ecology Letters*, 16(1):  
516 2230, 2013.

M. Plummer. Jags: A program for analysis of bayesian graphical models using gibbs sampling. In  
518 *Proceedings of the 3rd International Workshop on Distributed Statistical Computing (DSC  
2003)*. March, pages 20–22, 2003.

520 M. Plummer. *rjags: Bayesian graphical models using MCMC*, 2013. URL  
<http://cran.r-project.org/web/packages/rjags/index.html>. R package  
522 version 3.10.

R Development Core Team. *R: A Language and Environment for Statistical Computing*. R  
524 Foundation for Statistical Computing, Vienna, Austria, 2008. URL  
<http://www.R-project.org>. ISBN 3-900051-07-0.

526 J. R. Rohr, A. P. Dobson, P. T. Johnson, A. M. Kilpatrick, S. H. Paull, T. R. Raffel,  
D. Ruiz-Moreno, and M. B. Thomas. Frontiers in climate change–disease research. *Trends in  
528 ecology & evolution*, 26(6):270–277, 2011.

S. Ryan, A. McNally, L. Johnson, E. Mordecai, K. Paaijmans, and K. Lafferty. Climate change  
530 and malaria shifts: new implications for health geography and targeting control. Submitted.

A. Siraj, M. Santos-Vega, M. Bouma, D. Yadeta, D. R. Carrascal, and M. Pascual. Altitudinal  
532 Changes in Malaria Incidence in Highlands of Ethiopia and Colombia. *Science*, 343(6175):  
1154–1158, 2014.

534 E. D. Sternberg and M. B. Thomas. Local adaptation to temperature and the implications for  
vector-borne diseases. *Trends in Parasitology*, 30(3):115–122, 2014.

536 **Supplementary Appendix A:** Data sources, functional forms, default and informative prior  
details, equations for sensitivity analysis.

538 **Supplementary Appendix B:** Plots for full results for all components of  $R_0$ .

**Supplementary Appendix C:** Further results for  $R_0$  and sensitivity to temperature.

540 **Supplementary Files:** Compiled data, source code for analyses, and output files to reconstruct  
the analysis described in the manuscript.

Parameter	Definition	Functional Form
$a$	bite rate (1/ gonotrophic cycle length)	Briere
MDR	mosquito development rate	Briere
$p_{EA}$	egg to adult survival	quadratic
EFD	fecundity (eggs/female/day)	quadratic
$\mu$	mosquito mortality rate	quadratic
$bc$	vector competence	quadratic (and Briere)
PDR	parasite development rate (1/EIP)	Briere

Table 1: Component parameters of  $R_0$  and their definitions.

542 Figure 1: Posterior mean (solid line) and 95% credible interval (dashed lines) of the thermal  
 responses for all components of  $R_0$ , with informative priors together with the main data. Traits  
 544 modeled with a Briere thermal response ( $cT(T - T_0)\sqrt{(T_m - T)}$ ) are grouped in the top row,  
 concave-down quadratic ( $f(T) = a(T - T_0)(T - T_m)$ ) in the middle row, and concave-up  
 546 quadratic ( $aT^2 + bT + c$ ) in the bottom row. Data symbols correspond to the species of mosquito  
 or parasite used for the analysis. ●: *An. gambiae* or *P. falciparum* in *An. gambiae*; +: other  
 548 Anophelene species or *P. falciparum* in other Anophelene species; ×: *Aedes* species; ○: *P. vivax*  
 in other Anophelene species.

550 Figure 2: (TOP) Relative  $R_0$  ( $R_0$  divided by the maximum value of the posterior mean) assuming  
 a quadratic function for vector competence, with uninformative priors on all components (blue,  
 552 dashed) and informative priors on components (red, solid). 95% HPD around each curve are  
 shown as dotted lines. (BOTTOM) Smoothed posterior distributions of the (left) lower  
 554 temperature limit of  $R_0$ , (middle) peak temperature of  $R_0$ , (right) upper temperature limit of  $R_0$   
 all assuming a quadratic function for vector competence. Case with uninformative prior is shown  
 556 as a blue dashed line and with informative prior as a solid red line.

Figure 3: (a) Relative width of the 95% HPD intervals due to uncertainty in each component,  
 558 compared to uncertainty in  $R_0$  overall. Each curve was obtained as followed. For each  
 component,  $R_0$  was calculated for the thinned posterior samples of that component, with all other  
 560 components set to its posterior mean. Then the width of the inner 95% HPD was calculated at  
 each temperature. This was then normalized to the width of the HPD of the full posterior  
 562 distribution of  $R_0$  at each temperature. (b) Relative width of the 95% HPD in  $\left(\frac{dR_0}{dT}\right)_\theta$  scaled by the  
 width of the 95% HPD for  $\frac{dR_0}{dT}$  at each temperature, calculated as in (a). In both, a quadratic  
 564 response for vector competence (bc) was used.



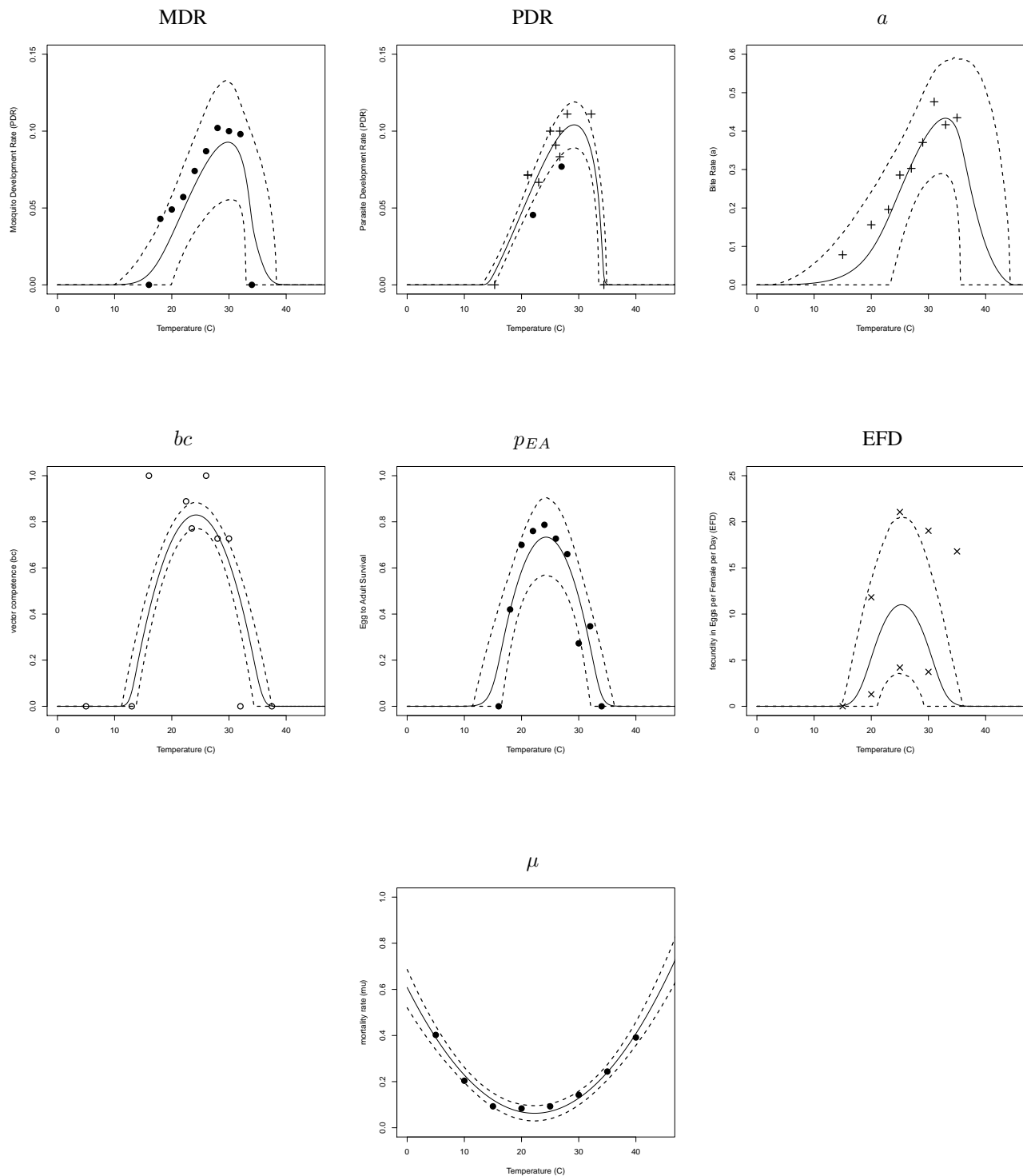


Figure 1: Posterior mean (solid line) and 95% credible interval (dashed lines) of the thermal responses for all components of  $R_0$ , with informative priors together with the main data. Traits modeled with a Briere thermal response ( $cT(T - T_0)\sqrt{(T_m - T)}$ ) are grouped in the top row, concave-down quadratic ( $f(T) = a(T - T_0)(T - T_m)$ ) in the middle row, and concave-up quadratic ( $aT^2 + bT + c$ ) in the bottom row. Data symbols correspond to the species of mosquito or parasite used for the analysis. ●: *An. gambiae* or *P. falciparum* in *An. gambiae*; +: other Anophelene species or *P. falciparum* in other Anophelene species; ×: *Aedes* species; ○: *P. vivax* in other Anophelene species.

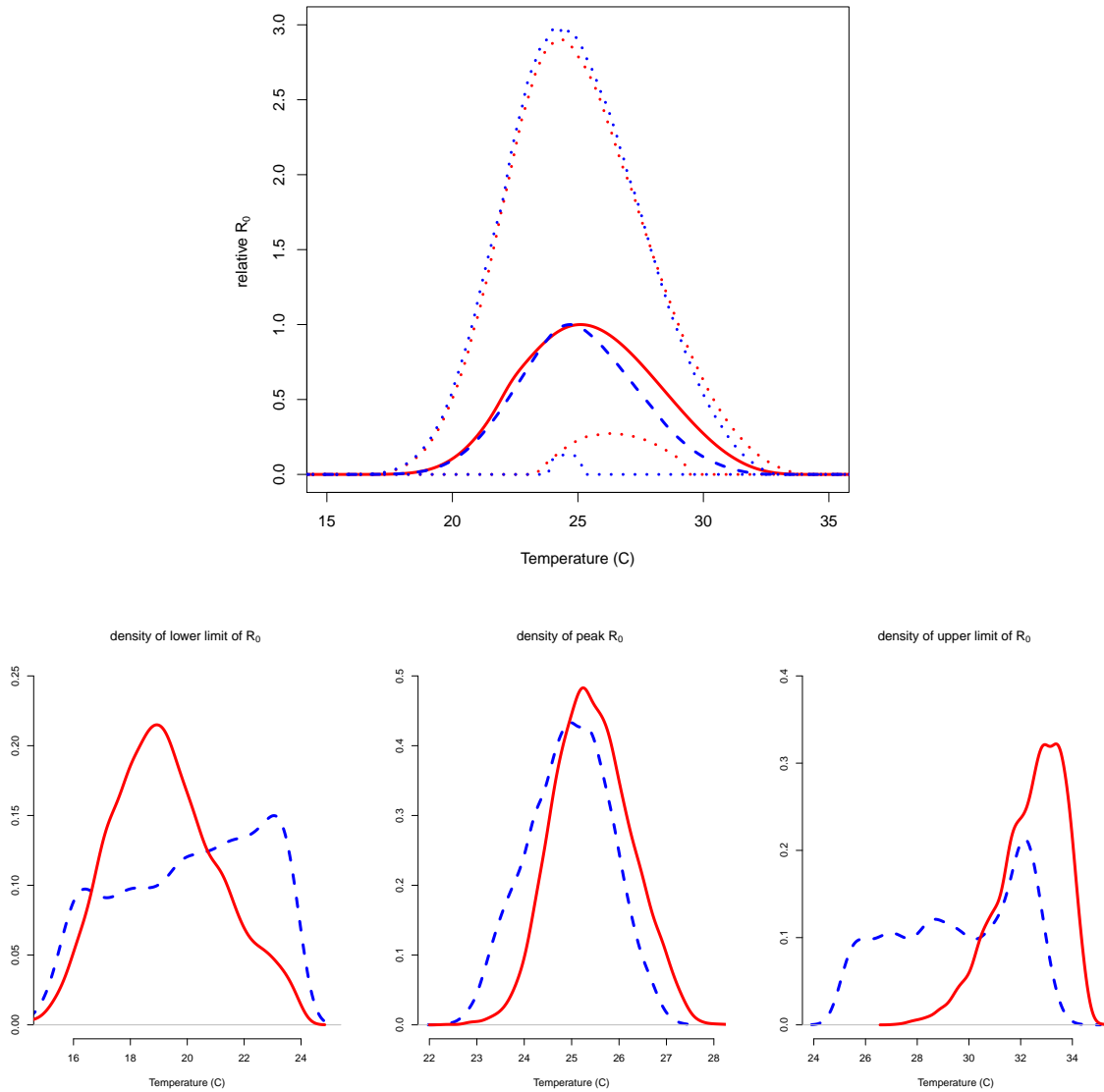
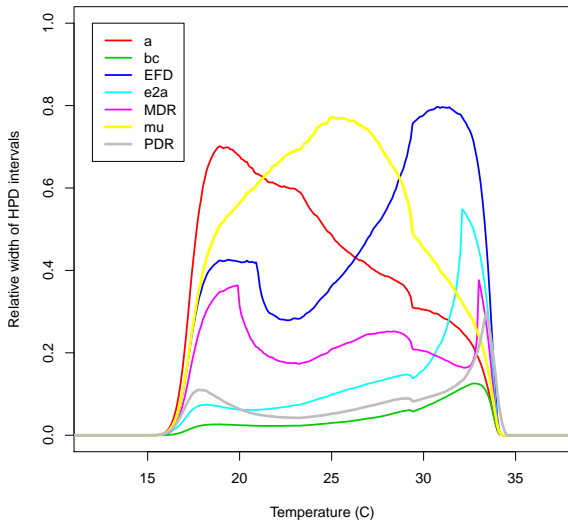
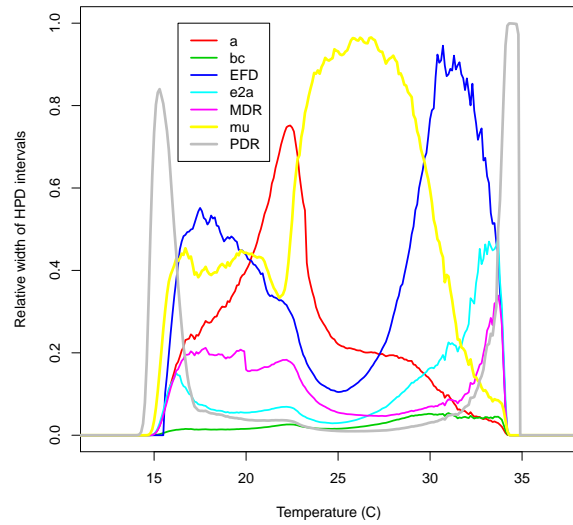


Figure 2: (TOP) Relative  $R_0$  ( $R_0$  divided by the maximum value of the posterior mean of  $R_0$ ) assuming a quadratic function for vector competence, with uninformative priors for all components (blue, dashed) and informative priors for all components (red, solid). 95% HPD around each curve are shown as dotted lines. (BOTTOM) Smoothed posterior distributions of the (left) lower temperature limit of  $R_0$ , (middle) peak temperature of  $R_0$ , (right) upper temperature limit of  $R_0$  all assuming a quadratic function for vector competence. Case with uninformative prior is shown as a blue dashed line and with informative prior as a solid red line. The height of the distribution indicates the relative probability of the value of the quantity of interest.



(a)



(b)

Figure 3: (a) Relative width of the 95% HPD intervals due to uncertainty in each component, compared to uncertainty in  $R_0$  overall. Each curve was obtained as follows. For each component,  $R_0$  was calculated for the thinned posterior samples of that component, with all other components set to its posterior mean. Then the width of the inner 95% HPD was calculated at each temperature. This was then normalized to the width of the HPD of the full posterior distribution of  $R_0$  (incorporating the full posterior samples from all components simultaneously) at each temperature. (b) Relative width of the 95% HPD in  $(\frac{dR_0}{dT})_\theta$  scaled by the width of the 95% HPD for  $\frac{dR_0}{dT}$  at each temperature, calculated as in (a). In both, a quadratic response for vector competence ( $bc$ ) was used.